 CMES, vol.2, no.1, pp.1-13, 2001

Three dimensional BEM and FEM stress analysis of the human tibia under pathological conditions

C.M. Müller-Karger[1], C.González[2], M.H.Aliabadi[3], M.Cerrolaza[4]

Abstract: In this paper, a three-dimensional Boundary Element model of the proximal tibia of the human knee is described and stresses and displacements in the tibial plateau under static loading are computed. The geometry is generated via three-dimensional reconstruction of Computerized Tomographies and Magnetic Resonance Imaging. Various models of different lengths from the tibia plateau are calculated. The BEM results are compared with a Finite Element model having the same geometry and tibia FE models available in the literature. Also reported are investigations of some pathological situations, including fractures. The results of the comparisons show that BEM is an efficient and suitable numerical technique for bone structure modeling.

keyword: 3D BEM, Biomechanics, Human Tibia Analysis

1 Introduction

To date, most of the work reported have dealt with knee joints, mainly the tibio-femoral joint, and some on the patello-femoral joint, but only few attempts have been made to calculate the mechanical behavior of the knee components in its physiological conditions [Hirokawa (1993), Hefzy and Grood (1988)]. Many finite element models reported in the literature are associated to the total knee replacement. They model the tibia plateau after a total knee replacement surgery. In this paper, the tibia in its intact, physiologically normal state is analyzed. A comparison between a normal, pathological and post-operative analysis of the joint may be used to determine appropriate prosthetic design, implant efficiency, surgical alignment and surgery success as well.

Several models of different length human-tibia-plateau are presented to determine the appropriate portion of the tibia to be included in a joint knee model.

Synovial joints are intricate geometrical structures composed by nonhomogeneous, anisotropic, nonlinear, viscoelastic materials. The loading conditions are still under investigation, therefore their magnitudes and directions are only approximately known. For comparison purposes, the loads considered in this investigation were taken from the literature [Hayes, Swenson, and Schurman, (1978), Little, Wevers, Siu, and Cooke (1986)]. The mechanical analysis was performed with the Boundary Element Method and the Finite Element Method.

For this model the bone geometry was built up by using Computerized Tomographies and Magnetic Resonance Imaging.

It is also possible to study the pathological situation of the tibial plateau with the platform develop in this research. To simulate the knee misalignments different load conditions with varus and valgus deformations might be applied to the model. One of the most common fractures of the tibial medial plateau is analyzed. Results of the mechanical behavior of the pathological system are presented and compared with the physiological model.

2 Previous Work

One of the earliest models published of the tibia was probably developed by Hayes, Swenson and Schurman (1978). They presented an axisymmetric finite element model to predict stresses and displacements in the tibia component of the human knee. They used a frontal section of a normal lateral tibia plateau from a 22-year-old autopsy specimen to generate the axisymmetric geometry and Fourier expansions to provide localized loading over the assumed joint contact forces. A resultant

[1] Department of Mechanical Engineering, Simón Bolívar University, Caracas, Venezuela. Email: cmuller@usb.ve
[2] Universitary Hospital, Faculty of Medicine, Central University of Venezuela, Caracas, Venezuela
[3] Department of Engineering, Queen Mary College, University of London, UK. Email: m.h.aliabadi@qmc.ac.uk
[4] Bioengineering Center, Faculty of Engineering, Central University of Venezuela, PO Box. 50.361, Caracas 1050-A, Venezuela. Email: mcerrola@reacciun.ve

force of 445 N was applied to the contact region of the femoral condyles with the articular cartilage. To account for the large differences in the material properties of the synovial components, they considered four separate material regions: a) compact bone in the cortical diaphysis and in the methaphyseal shell; b) articular cartilage; c) subcondral trabecular bone; and d) intramedullary trabecular bone. Materials properties were estimated from the literature [Hayes and Mockros (1970), Evans (1973, McElhaney (1970)]. Results indicated that most of the load applied to the cartilage surface of the tibia, was distributed to the compact bone of the tibia diaphysis, through the trabecular bone. Hayes, Swenson, and Schurman, (1978), also presented (based on their model) a hypothesis concerning the pathomechanics of the tibial plateau fractures. Their finite element model predicts both high compressive normal stress and high shear stresses in the subchrontal trabecular bone. They found that regions of maximum shear stress correspond closely to the initiation sites for split fractures of the plateau. Their hypothesis suggested that fracture morphology is governed by the stress-strength relations for subchondral trabecular bone rather than by the pattern of load application to the knee, this implied that both axial and abduction load results in similar stress distribution in the tibial plateaus and that the initiation site for compression fractures is related to the region of maximum compressive stress predicted by the model. Similarly, the initiation site for split fractures is related to predicted regions of high shear stress.

Murace, Crowninshied, Peterson, and Chang (1983) developed an axisymmetric model of proximal tibia and tibia components, to study the problems associated with total knee replacement. A finite element analysis was performed on the model based on nonaxisymmetric loading condition, with different load applied to the medial and lateral condyles.

Little, Wevers, Siu and Cooke (1986) developed a three dimensional finite element model of the proximal tibia to provide a base line for further modeling of prosthesis resurfaced tibia. The geometry for the model was developed by digitizing coronal and transverse sections made with the milling machine, from one fresh tibia of average size. An indentation test was used to measure the stiffness and the ultimate strength of the cancellous bone, and all materials were assumed to be linearly elastic and isotropic. They used a load condition of 2450 N [Harrington (1976)], which occurs during normal gait at the stance phase in near full extension. The load was distributed over the nodes at the top of the cartilage areas with the highest load in the center of the medial and lateral areas. The load distribution follows approximately a trapezoidal pattern. Results were compared with strain gauge tests and with a two-dimensional axisymmetric finite element results found in the literature. Qualitative comparison between trabecular alignment, and the direction of the principal compression stresses in the cancellous bone, were shown to be in good agreement.

Metha and Rajani (1995) constructed a 3D solid model of the human tibia and fibula using Magnetic Resonance Imaging and solid modeling software. They conducted a finite element analysis of the tibia to evaluate stresses under static loads and to study the effect of varying material properties on these stresses. Two finite element models were developed. The first model took into consideration 130 mm length of the tibia from the tibia plateau and the second for the entire length of the tibia. Each one of the above models was analyzed using either one, three and four materials for different areas of the bone. Their first model was assumed to be made up entirely by compact bone, the second model was a 130 mm length tibia composed by a cartilage layer, compact bone and cancellous bone, the last model include subchondral trabecular bone and intramedullary trabecular bone. Loading conditions and material properties were the same as those used by Hayes et. al (1978). They obtained maximum stresses developed for cancellous bone within ultimate stress values. They also found a large area of stress concentrations in the region, even below 130 mm from the tibial plateau, which proved the importance of analysing the whole tibia when conducting studies on lower extremities of the human body.

Mierendorff and Mathias (1998) presented a finite element model to investigate the internal stresses generated within the tibia after impact loads. A three-dimensional FE model of the tibia was developed using information obtained from Magnetic Resonance Images. The cortical bone had linear, isotropic and homogenous material properties and the model neglected the associated soft tissues and fatty marrow into the medullar canal. A block was allowed to free-fall onto the shaft of the tibia, simulating an impact load. The tibia is a long, dense, tubular bone and this shape and flexibility of this bone seemed to indicate that stress was quickly dispersed throughout the length of the bone.

Watanabe, Ayokoyama, Hirai and Hirasawa (1998) studied the mechanism of lateral-tibial-plateau fractures analyzed by dispersion of stress waves. Their study was designed to evaluate stress-wave dispersion after impact loading by numerical methods, in order to explain the mechanism of lateral plateau fractures.

Hyodo, Yamada Tateishi (1998) applied a thermoelastic stress analysis to the human tibia. This analysis is a non-contact technique which uses the thermoelastic qualities of hard tissues such as bone which enables easy measurements and imaging of the distribution of principal surface stresses. Using this approach, they performed stress analysis of human tibias in simulated loading conditions at various modes of varus valgus loading on the knee joint. Thermoelastic stress images were demonstrated in medial, lateral and posterior aspects of the tibia. In normal loading conditions, when the knees are considered to be aligned, they obtained that the majority of the high stress regions were concentrated in the posterior part of the tibia. The epiphysis of the proximal tibia, which consists predominantly of cancellous bone, showed tensile stress and the diaphysis, which consist of compact bone, showed compressive stress in every plane. Hyodo et al demonstrated also that small changes in the alignment of the knee joint could have great influences on the stress pattern of the proximal tibia.

3 The Human Tibia Model

The lower leg portion is made up with two bones, the medial tibia and the lateral fibula. The fibula is a long-slender bone, having its head articulated with the tibia by an interosseous membrane that fills the gap between the bones. The fibula does not take part in the knee-joint and supports no weight, therefore it will not be considered in this analysis.

The proximal end of the human tibia displays very special characteristics; it is form by the superior base of a truncated cone. The plateau presents two condyles, internal (medial) and external (lateral), which articulated with the medial and lateral condyles of the femur respectively. Between the condyles there is an intermediate area (the tibial thorns) which do not participate in the contact between the bones. The external plate is smaller but higher than the internal one, displaying a convex shape. The internal plate is concave. On these plates and toward their

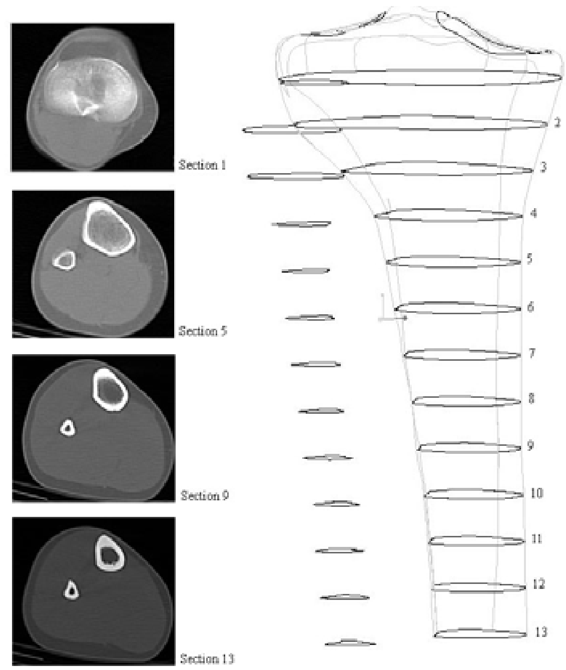

Figure 1 : Ct. and 3D wireframe reconstruction of the tibia

borders, one can find out some cartilaginous structures denominated meniscuses. Going down, the tibia narrows into the diaphysis, which is also called the shaft of the tibia, and then expands again towards the distal end of the tibia that articulates the ankle.

The tibia is a long hollow bone, which has an expanded metaphysis and an epiphysis at both ends of a thick-walled tubular diaphysis. It is a complex structure composed of cancellous (trabecular) bone, cortical (compact) bone and articular cartilage. The mechanical properties of these components have been extensively studied and several reports are available in the literature [Buckwalter, Glimcher, Cooper and Recker, (1995)]. Cortical and cancellous bone have the same matrix composition and structure, but the cortical bone has a much less porosity matrix (1:5) than the cancellous bone. The modules of elasticity and the ultimate compressive strength of cortical bone may be as much as ten times greater than those of a similar volume of cancellous bone. Cortical bone forms approximately 80% of the mature skeleton and surrounds marrow and cancellous bone plates [Recker (1992)]. In long or hollow bones, dense cortical bone forms the diaphysis, and there is little or no cancellous bone in this region. The thick cortical walls of the dia-

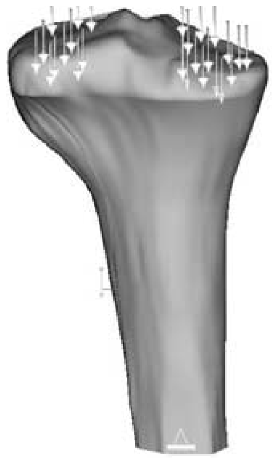

Figure 2 : Rendered model and loading conditions

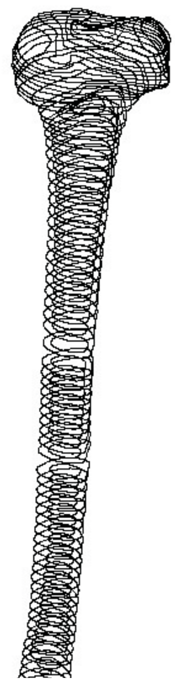

Figure 3 : Wire frame model of the whole tibia

physis become thinner and increase in diameter as they form the metaphysis, where plates of cancellous bone orient themselves to provide support for a thin shell of subchondral bone that underlies the articular cartilage. Although cortical and cancellous bone has the same composition, the difference in the distribution of the material is responsible for the differences in the mechanical properties. In long bones, the thick, dense tubular cortical bone of the diaphysis provides maximum resistance to torsion and bending. In the metaphysis and epiphysis, the thinner corticals and subchondral bone supported by cancellous bone allow higher deformation to occur under the same load.

3.1 Geometry Modeling

Various models of the tibia were developed using Computerized Axial Tomographies (CT) and Magnetic Resonance Imaging (MRI). CT provides many advantages in bone modeling (Marom et. al. 1990). If CT scanner are properly calibrate the acquired images of the bone cross section provide accurate information about the structure geometry and the apparent density of bone tissue. The CT are images composed by pixels of different gray scale, a segmentation process consist in determining the bone external geometry by considering all the CT pixel points with the same gray value.

For the first model, images of a healthy 32–years-old female were used. The available CT and MRI images cover a portion up to 135 *mm* below the plateau of the tibia, having a 78 *mm* average top-diameter. The Computerized Tomographies were converted to the Tag Image File format (TIF) using a commercial software (OSIRIS, 1998). A three dimensional wireframe structure was constructed using both Imaging Techniques. Thirteen (10 *mm* thick) axial CT slides were used to reconstruct the shaft and the proximal portion of the bone, as shown in figure 1.

Ten (4 *mm* thick) MRI slices in transverse direction were used to reconstruct the tibia plateau, the MRI in the perpendicular direction were also used to improve the major feature changes displayed by the proximal surface of the plateau. In this case, the images were imported directly into the parametric Software Pro/Engineer (1998) and the boundaries of the bone of each slice were defined by pixels of the same gray scale using splines. This software was used for the 3D modeling and reconstruction of the rendered model. A solid protrusion was generated based on the axial boundary-wireframe structure as shown in Figure 2.

Several other models were generated using 1-*mm*-thick CT images of the male from the "Visible Human Project" (1999). In these cases, MRI images were not necessary. In order to reproduce appropriately the tibial plateau the concentration of images used in the proximal tibia was higher than the one used in the shaft of the tibia, as

Figure 4 : Model with intramedular cavity

shown in figure 3. These three models were designed considering the intra medullar cavity, as shown in figure 4. The segmentation process was performed in this case using the software Surfdriver (1999), which directly defines the border of the bone by pixels of the same gray scale. The wire frame structure created with Surfdriver was imported in Pro-Engineer using the IGES format.

3.2 Material Properties and loading Conditions

The knee transmits different forces as: the body weight it supports, the muscle forces acting across it, and other forces during movement because the body segments connected by the joint are being accelerated. [Freeman (1980)]. In symmetrical two-legged standing, no muscle are acting and each tibio-femoral joint theoretically transmits a half of the bodyweight above the knees, and in one leg standing one knee would transmit the whole weight. When walking or carrying out other activities where the muscles act, the transmitted forces can be as high as to 7.1 times the body forces. In general the muscular forces, and hence the joint forces, will be much larger than the weights. Resultant knee-joint force has been estimated (Seireg and Arvikar, 1973) to range from 0.5 times the bodyweight during two-legged, upright stance, up to 4 to 7.1 times bodyweight during normal walking. Morrison (1968) has shown that the maximum joint loading occurs during the stance phase only. Swing phase loading is small and it is due entirely to effects of gravity and inertia acting on limb segments. Harrington (1976) simplified the joint force analysis by neglecting inertia forces, on the basis that the forces at the joints of the leg are larger during the stance phase of walking, when the accelerations are less important, than in the swing phase. For activities such as rising from a chair or stair climbing, it is customary to neglect inertia forces. In his research, Harrington (1976) found three peak loads that corresponded to hamstring, quadriceps and gastrocnemius force actions. The relative magnitude of the peak varied for different subjects but exhibited similar characteristics for each individual repeated tested. The average maximum bearing force transmitted to the knee was 3.5 times the body weight in the quadriceps force action. The center of joint pressure for all normal subjects was found (Harrington 1976) to be located in the medial joint compartment throughout most of the stance phase.

Two loading conditions are studied in this paper. The first, (Hayes, Swenson and Schurman, 1978), is an axisymmetric total load of 890 *N*, distributed in equal loads of 445 *N* applied to each plateau. The second, (Little, Wevers, Siu and Cooke, 1986) occurs during normal gait at the stance phase in near full extension with a magnitude of 2450 *N*. The loaded nodal points covered areas approximately equal to the following contact areas (Kettlekcamp and Jacobs, 1972) of 468 mm^2 (medial condyle) and 297 mm^2 (lateral condyle). The compressive force was distributed over the nodes at the tibia condyles as a constant distributed force. The surface at the base of the model has been restrained into the three translational degrees-of-freedom, thus representing a rigid boundary at the distal part of the model. This research is a first approach to this subject and does not consider the differences in the material properties of the synovial components. In the first model the proximal tibia is taken as solid bone composed only of compact bone. In the following examples the tibia is considered as bone composed only by cortical bone having an intra-medullary canal. Compact bone is assumed to be linear, perfectly elastic and transversally isotropic with a Poisson's ratio of 0.3. The Young modulus of the bone was assumed to be 17.2 *GPa*, [Reilly and Burstein (1974a,1974b), Carter and Hayes (1977) , Carter and Spengler (1978)].

Two groups of simulations are presented. The first is

Figure 5 : Boundary Element Mesh of (a) 135 *mm* model; (b) 227 *mm* model; (c) 227 *mm* model

made up by three models taken from images of the male from the Visible Human Project. These images correspond to the left knee. These three models were generated using different lengths from the tibial plateau, indeed 135, 270 and 360 *mm* respectively. The distances were chosen accordingly to the changes in the axial bone's curvature. These models were designed considering the intra medullar cavity. The boundary mesh is shown in figure 5. The model for the whole tibia (360 *mm*) results in 1920 nodes and 689 quadrilateral 8-node-surface elements, the partial model of 270 *mm* of length results in 1361 nodes and 498 elements and finally the model of 135 *mm* length results in 1045 nodes and 387 elements.

The second groups of models are built up by simulating a 135 *mm* long tibia in its normal stage and the fracture of the same model. The images of these simulations were taken from CT and MRI of the right knee of a healthy 32-years-old female. The results for this analysis were compared with a FE analysis of the exact same geometry. The final BE model results in 1146 nodes and 413 quadrilateral 8-node surface elements as shown in figure 6.

For all the models the solid bone were meshed with the subroutines of Pro-Engineer Software using Pro/MESH & Pro/FEM (1998). This was accomplished by establishing minimum and maximum size of the elements, avoiding excessively fine or coarse meshes. Very distorted el-

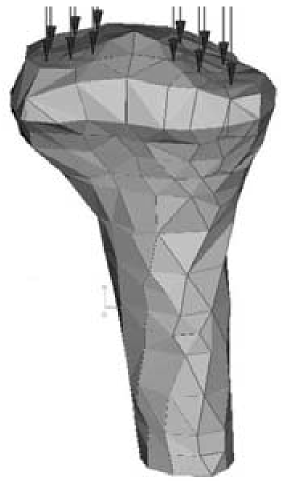

Figure 6 : BEM discretization: 1146 nodes and 413 elements

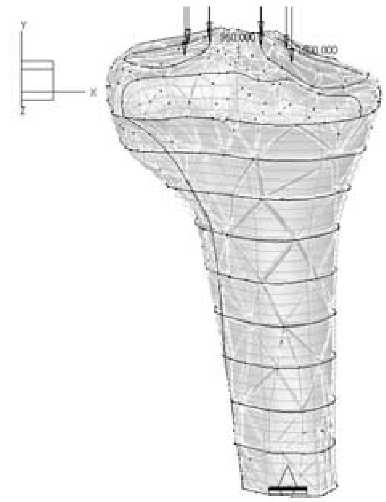

Figure 7 : FEM discretization: 1713 tetrahedral elements

ements were neglected.

3.3 Finite Element Model

For comparison purposes a Finite Element analysis was also performed with the same 135 *mm* model, using the commercial software Pro/MECHANICA (1998). The final model results in 1713 tetrahedral elements as shown in figure 7.

3.4 Boundary Element Model

The BEM analysis in this research was carried out using an in-house software. The code uses 8-noded isoparametric elements for modelling surface of the problem. The analysis was linear and elastic in this first step of the work. Direct and Von-Mises stresses as well as displacements are obtained on the surface of the model. The boundary mesh was exported into a neutral file and then imported by the BEM code.

Postprocessing results were done by using in part a graphic an in-house software software and in part with the postprocessor facilities of Pro-Engineer. Stress and displacement fields are also easily included into the model view by simply writing them into text files. The user can define a multi-window environment in order to display two-three or four simultaneous views.

4 Analysis of Human Tibia in Normal Conditions

4.1 Solid tibia Model Constituting of Compact Bone

The BEM analysis yields a maximum Von Misses stress developed in the tibia of 25.54 *MPa* in the distal part and 11 *MPa* in the upper tibia as shown in figure 8. The maximum displacement occurs in the lateral upper part of the tibia with a maximum value of 0.27 *mm*. This results compare very well with the FEM analysis as shown in figure 9 and 10, for maximum value of the Von Misses stress of 27.57 *MPa* and a maximum displacement of 0.246 *mm*.

Results reported by Little, Wevers, Siu and Cooke (1986) show a maximum compression stress of 24.77 *MPa* for a total load of 2450 *N*, for a model considering 4 different materials, and a maximum stress in the upper tibia of 8 *MPa*. Metha and Rajani (1995) obtained a maximum compressive stress of 7.37 *MPa* at approximately 60 *mm* from the distal end of the tibia. The stress results indicate compressive stress developing from the anterior to the posterior part of the model.

4.2 Three Models having different lengths and intermediary cavity.

The stresses in these models were comparatively higher that the previous model because the medullar cavity was taken into account. The maximum compressive stress in the model of 135 *mm* was 50.93 *MPa* and occurred at a

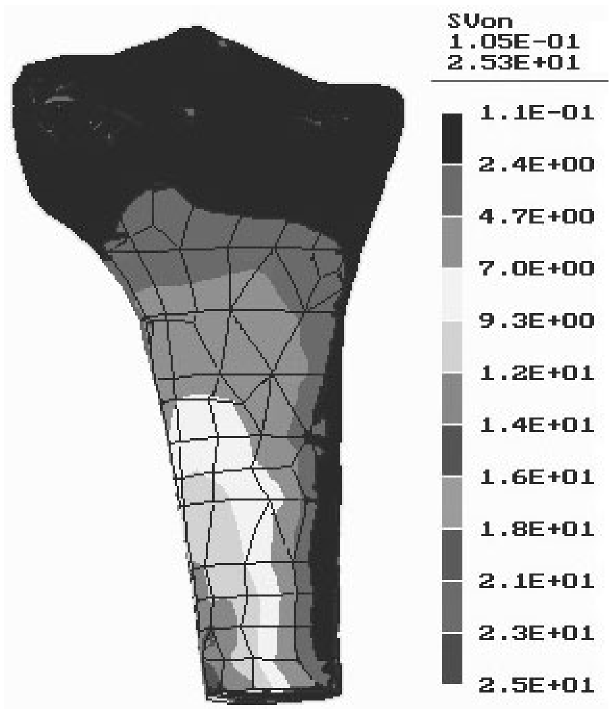

Figure 8 : Von Misses Stresses Calculated with BEM (MPa)

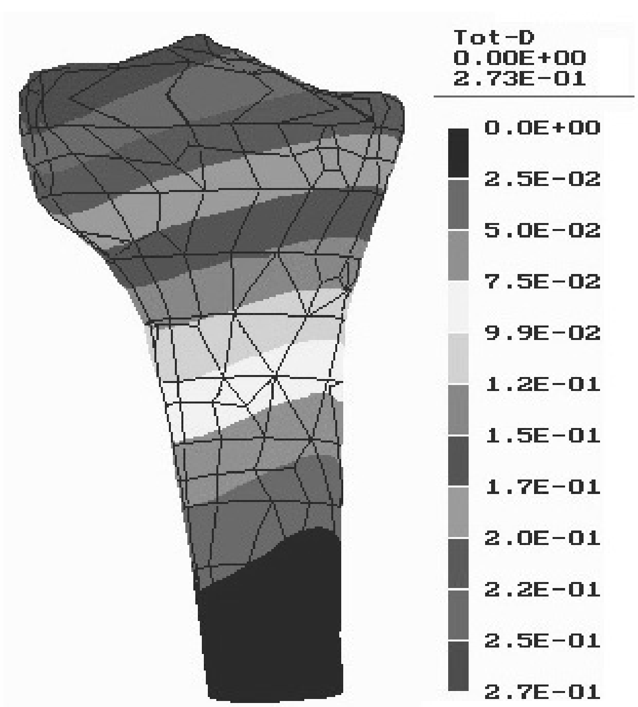

Figure 9 : Displacements calculated with BEM (mm)

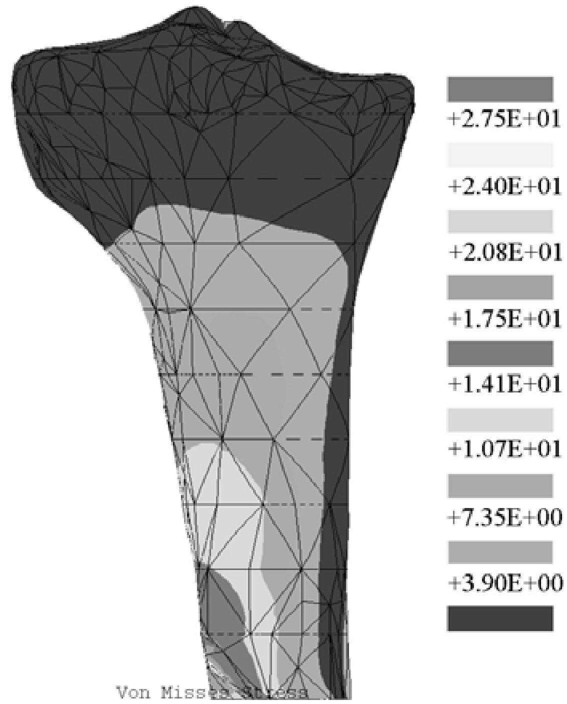

Figure 10 : Von Misses Stresses Calculated with FEM (MPa)

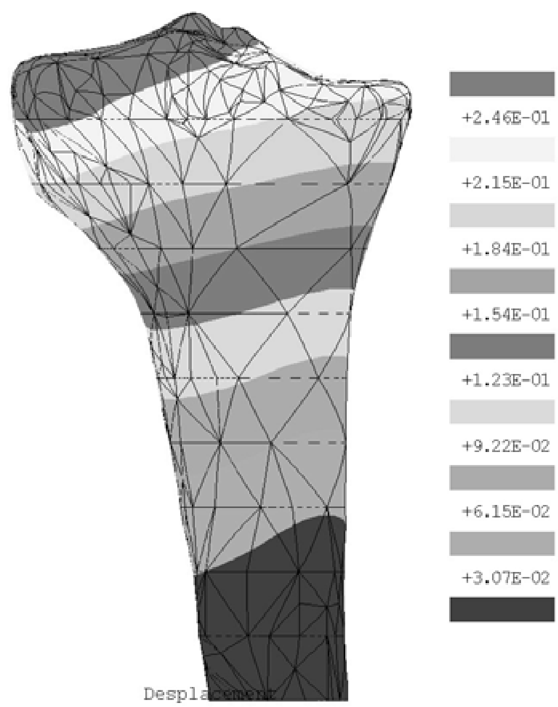

Figure 11 : Displacements calculated with FEM(mm)

distance of 130 *mm* from the tibial plateau in the posterior face of the bone (figure 13a). For the 270 *mm* length model the maximum compression stress was 54.7 *MPa* at a distance of 220 *mm* approximately, and it is important to notice that both sides of the bone displayed similar stresses (figure 13b). For the whole tibia model the maximum compression stress was 100.18 *MPa* and occurred at 330 *mm* approximately from the proximal part. The stresses at the whole tibia model were smoother and distributed along the tibia shaft, as shown in figure 13.c. A positive deflection towards the lateral direction increasing gradually to the upper part with a maximum displacement of 5.74 *mm* was observed (figure 12).

This result is in agreement with the results presented by Metha and Rajani (1995) and shows a lateral deflection of 7.954 *mm* for a model consisting of three materials. The displacement of the model presented here are comparatively lower as compact bone is considered. This behavior was expected for long or hollow bones. A similar behavior was reported by Rohlman, Mossner, Bergmann and Kölbel (1982) using finite element analysis of the femur with hip endoprosthesis. These results show that the stresses developed in the shorter models are different and considerably lower than the ones developed in the whole tibia, which shows the importance of modeling the whole length of the bone when conducting studies related to the knee joint or others in the lower extremity of the human body.

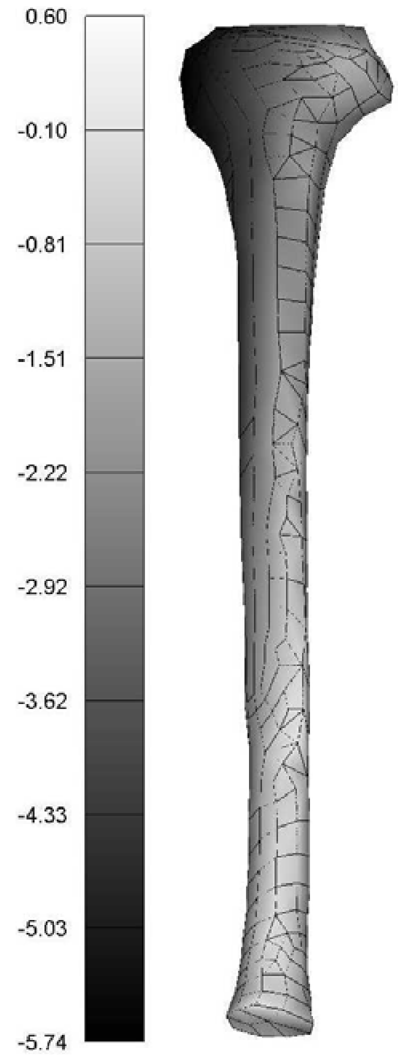

Figure 12 : Displacements in the z direction

5 Analysis of Tibial-Plateau Fractures

Strong valgus or varus forces combined with axial loading are believed to cause the proximal tibia-plateau fractures (Brower, Jupiter, Levine and Trafton, 1992), the magnitudes and direction of the forces determine the characteristics of the fractures:

1. Strong axial load with a deviation component in valgus
2. Strong axial load with a deviation component in varus
3. Excessive axial forces directed on both tibial plates.
4. Combination of all the above with torsion.

The internal structures of the knee are stronger than the external areas, due to the acting axial loads. For this reason, the external fractures are more frequent than the internal ones, and they occur in the cases of high impacts. Generally the damage associated of the soft parts, is as important as the bone fractures. During the installation to the total knee-prosthesis, some cases of fractures are presented by wrong handling of surgical instruments, as well as inappropriate treatment of the soft parts in weak-bone due to osteoporosis.

According to the AO classification (Muller Müller, 1990) the fractures in proximal tibias can be classified as (see figure 14): B1, Partial articular fracture, pure split. B2, Partial articular fracture, pure depression. B3, Partial articular fracture, split depression. C1, Complete articu-

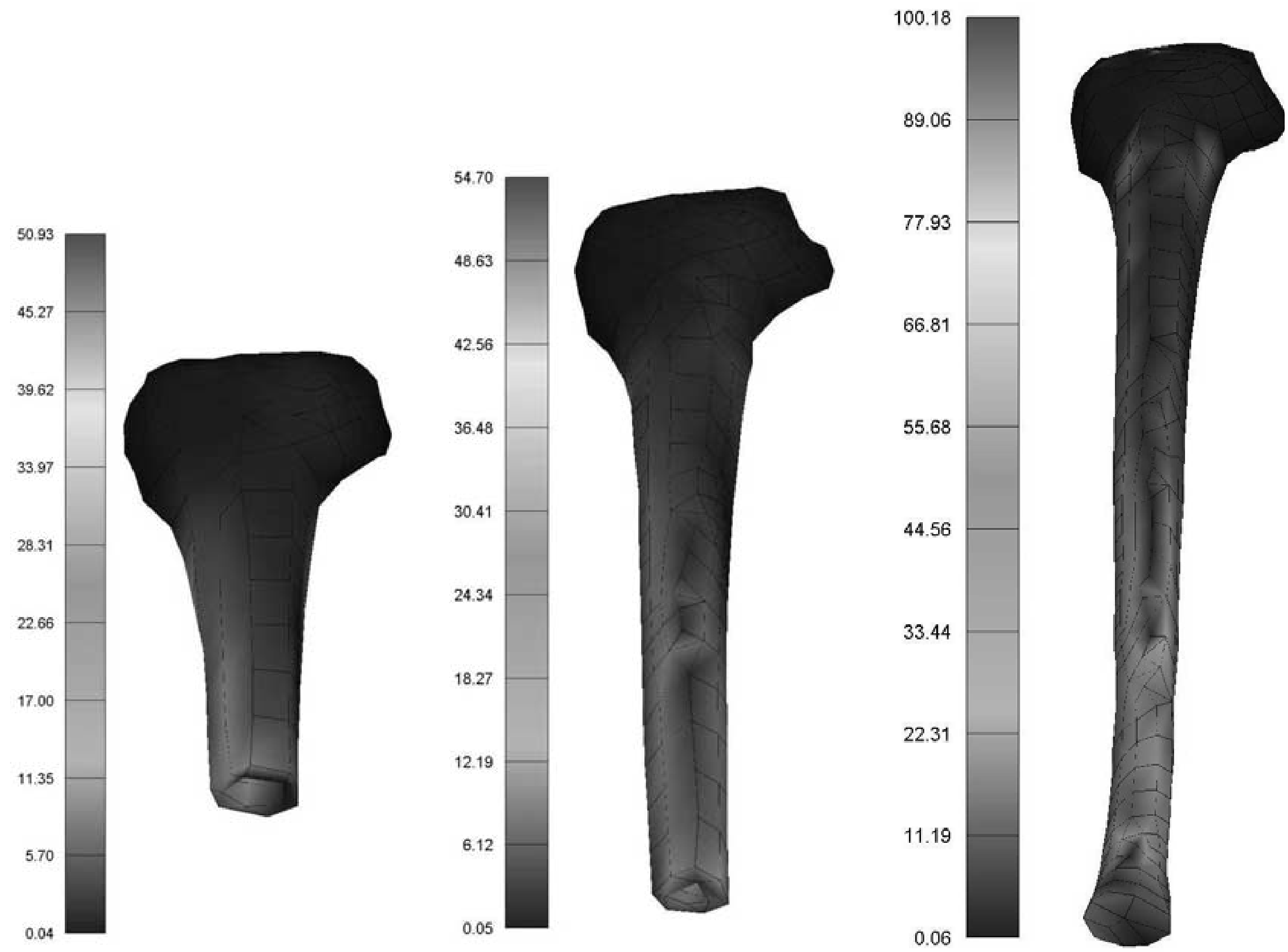

(a) (b) (c)

Figure 13 : Von Misses Stresses calculated with BEM: (a) 135 *mm* long model (*MPa*); (b) 227 *mm* long model (*MPa*); (c) 360 *mm* long model (*MPa*)

lar fracture, articular simple, metaphyseal simple. C2, Complete articular fracture, articular simple, metaphyseal multifragmentary. C3, Complete. Slip fractures are most common in young people, on the other hand isolated depressed fractures occurs in old people.

The results obtained for the physiological system show the region of maximum stress in the upper part of the lateral condyle. Therefore we choose a partial fracture of type B1. The rendered model of the fractured tibia is shown in figure 15, whereas figure 16 shows the BEM mesh of the fractured upper tibia with 1351 nodes and 468 elements. The BEM analysis gave a maximum stress of almost 100 *MPa* in the surroundings of the tip-crack as shown in figure 17. These results imply a total stress much greater that the maximum stress of the non-fracture bone.

6 Discussions and Concluding Remarks

Mechanical analyses have been applied mostly to joint replacement, often to study the interface between bone and implants. A better understanding of bone mechanics in its natural condition will give a more precise understanding of the system with intrusive components.

The first approach in this research was an axisymmetric load condition, which was used by Hayes, Swenson and Schurman (1978). Since the geometry used in this re-

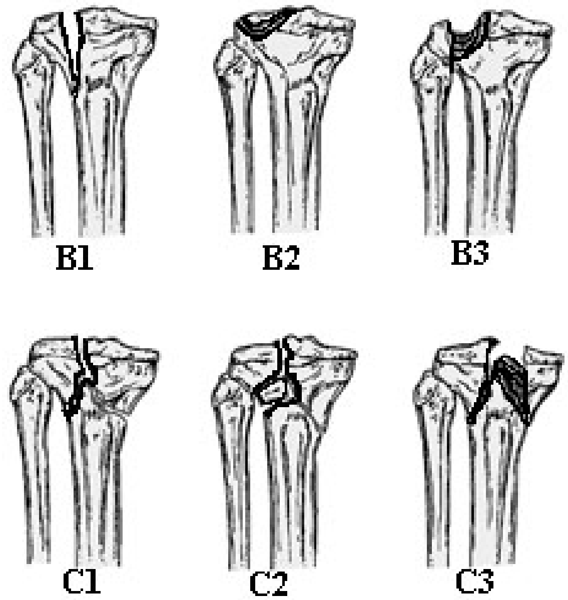

Figure 14 : The AO classification of fractures of proximal tibia

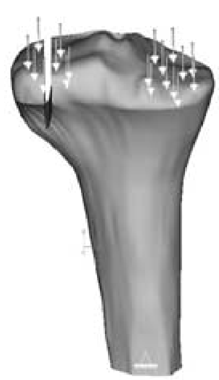

Figure 15 : Fractured Model of the Tibia

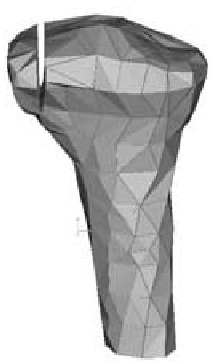

Figure 16 : BEM mesh of the fractured tibia

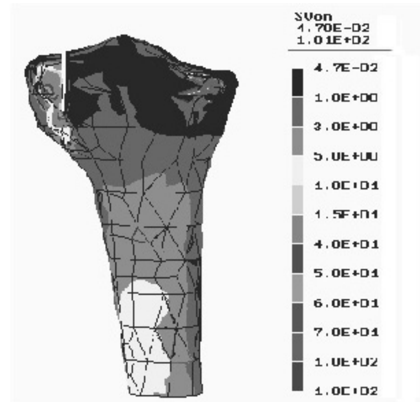

Figure 17 : Von Misses Stresses for the fractured tibia (MPa)

search is not axisymmetric, although it follows the real geometry of the tibia, the results with this load condition were not satisfactory. The compressive Von Misses stresses yield considerable higher values than those reported in the literature. Therefore a variation in the contact areas between the medial and the lateral plateaus was used. Kettlekamp and Jacobs (1972) reported contact areas ranging from 250 mm^2 up to 670 mm^2 for the medial plateau and from 170 to 510 mm^2 laterally. For the analysis presented here the contact areas used were 468 mm^2 medially and 297 mm^2 laterally. These loading conditions produced more reliable results and compared very well with other reported results.

The boundary element analysis uses much less elements to determine stresses and displacements. In this analysis the BEM model needed only 413 quadrilateral surface elements while the FEM analysis needed 1716 tetrahedrical elements. The BEM allows great flexibility in modifying the bone geometry without the need to reconstruct all the volume mesh. This is a very important advantage of BEM when simulating fractures of the bones.

The model presented here was assumed to be made up entirely of compact bone, except for the intra medullar cavity. The next step of this research is to refine the model by considering the bone to be composed by a compact bone shell, cancellous bone filling the areas within the compact bone, an articular cartilage surface over the tibia plateau and an intermedulary area with no material. A complete knee-joint model is a future goal, were the femur tibia joint can be modeled. For this purpose a contact analysis and the simulation of soft tissues is necessary. The ligaments origin and muscle insertions can be digitized form Magnetic Resonance images.

The analysis platform developed herein will be used to study several pathological conditions of the knee-joint and knee-replacements design. As suggested by Hayes, Swenson and Schurman (1978) the mechanics of the tibial plateau fractures is governed by the stress-strength relations. This implies that the initiation site for compression fractures is related to the region of maximum compressive stress predicted by the model. Similarly, the initiation site for slip fractures is related to the predicted region of shear stresses. The analysis presented here may result in a platform to study controlled tibia plateau fractures, to get a better understanding of the knee joint system.

Acknowledgement: The authors wish to acknowledge the support provided by University Simón Bolívar, the Council for Humanistic and Scientific Development of the Central University of Venezuela (CDCH) with the project N.08-314222-98, and the National Council for Scientific Research of Venezuela (CONICIT) for the grants provided for this research.

References

Brower, B. D.; Jupiter, J. B.; Levine, A. M.; Trafton, P. G. (1992): *Skeletal trauma: fractures, dislocations, ligamentuos Injures*. W.B. Saunders Company 2^nd Ed.

Buckwalter, J. A.; Glimcher, M. J.; Cooper, R. R.; Recker, R. (1995): Bone biology. part i: Structure, blood supply, cells, matrix, and mineralization. *Journal of bone and Joint Surgery*, vol. 77A, no. 8, pp. 1256–1275.

Carter, D. R.; Hayes, W. C. (1977): The compressive behaviour of bone as a two-phase porous structure. *Journal of Bone and joint Surgery*, vol. 59a, pp. 954–962.

Carter, D. R.; Spengler, W. C. (1978): Mechanical properties and composition of cortical bone. *Clinical orthopeadics and Related Research*, vol. 135, pp. 192–214.

Evans, F. G. (1973): *Mechanical Properties of the Bone*. Charles C. Thomas, Springfield, IL.

Freeman, M. A. R. (1980): *Arthritis of the Knee, Clinical Features and Surgical Management*. Spinger Verlag, Berlin Heildelberg, New York.

Harrington, L. J. (1976): A bioengineering analysis of force actions at the knee in normal and pathological gait. *Journal of Biomedical Engineering*, vol. 11, pp. 167–172.

Hayes, W. C.; Mockros, L. F. (1971): Viscoelastic properties of human articular cartilage. *J. appl. Physiol.*, vol. 31, pp. 562–568.

Hayes, W. C.; Swenson, L. W.; Schurman, D. J. (1978): Axisymmetric finite element analysis of the lateral tibial plateau. *Journal of Biomechanics*, vol. 11, pp. 21–23.

Hefzy, M. S.; Grood, E. S. (1988): Review for knee models. *Applied Mechanics Review*, vol. 41, no. 1, pp. 1–13.

Hirokawa, S. (1993): Biomechanics of the knee joint: A critical review. *Critical Rev. Biomedical Engineering*, vol. 21, pp. 79–135.

Hyodo, K.; Yamada, M.; Tateishi, T. (1998): Thermoelastic stress analysis of human tibia. In *Proceeding of Third World Congress of Biomechanics*. August 2-8, Sapporo, Japan.

Kettlekcamp, D. B.; Jacobs, A. W. (1972): Tibiofemoral contact area-determination and implantations. *Journal of Bone and Joint Surgery*, vol. 54A, pp. 167–172.

Little, R. B.; Wevers, H. W.; Siu, D.; Cooke, T. D. V. (1986): A three dimensional finite element analysis of the upper tibia. *Journal of Biomechanical Engineering*, vol. 108, pp. 111–119.

Marom, S. A.; Linden, M. J. (1990): Computer aided stress analysis of long bones utilizing computed tomography. *J. Biomech.*, vol. 23, no. 5, pp. 399–404.

Mc Elhaney, H. H.; Alem, N. M.; Roberts, V. L. (1970): A porous block model for cancellous bone. In *ASME Pub. 70-WA/BHF-2*. New York.

Metha, B. V.; Rajani, S. (1995): Finite element analysis of the human tibia, computer simulations in biomedicine. In H. Power., R. H.(Ed): *Computational Mechanics Publications*, pp. 309–316.

Mierendorff, S.; Mathias, K. J. (1998): Dynamic loading of the tibia: A finite element study. In *Proceeding of Third World Congress of Biomechanics*. August 2-8, Sapporo, Japan.

Morrison, J. B. (1968): Bioengineering analysis of force actions transmitted by the knee joint. *Biomedical Engineering*, vol. 3, pp. 164.

Müller, M. E. (1990): *The Comprehensive Classification of Fractures of Long Bones*. Berlin, Springer-Verlag.

Murace, K.; Crowninshied, R. D.; Peterson, D. R.; Chang, T. (1983): An analysis of tibia component design in total knee arthroplasty. *Journal of Biomechanics*, vol. 16, pp. 13–22.

OSIRIS (1998): *Imaging Software, User Manual version 3.1*. Hôpital Universitaries de Geneve.

Pro/ENGINEER (1998): *Fundamentals User Guide, Release 20.0*. Parametric Technology Corporation.

Pro/FEM, P. . (1998): *User's Guide, Release 20.0*. Parametric Technology Corporation.

Project, V. H. (1999): *http://Vhd_mms.cilea.it/*.

Pro/MECHANICA (1998): *Using Structure with Pro/Engineer, Release 20.0*. Parametric Technology Corporation.

Recker, R. R. (1992): Embryology, anatomy, and microstructure of bone. In Coe, F. L.; Favus., M.(Eds): *Disorders of Bone and Mineral Metabolism*, pp. 219–240. New York, Raven Press.

Reilly, D. T.; Burstein, A. H. (1974): The elastic modulus for bones. *Journal of Biomechanics*, vol. 17, pp. 271–275.

Reilly, D. T.; H., B. A. (1974): Mechanical properties of cortical bone. *Journal of Bone and Joint Surgery*, vol. 56A, pp. 1001–1022.

Rohlman, A.; Mossner, U.; Bergmann, G.; Kölbel, R. (1982): Finite element analysis and experimental investigation in the femur with hip endoprosthesis. *Journal of Biomechanics*, vol. 16, pp. 727–742.

Seireg, A.; Arvikar, R. J. (1973): A mathematical model for evaluation of forces in lower extremities of the musculoskeletal system. *Journal of Biomechanics*, vol. 6, pp. 313–326.

Surfdriver (1999): *http://Surfdriver.edu.eu.org/contact.html*.

Watanabe, Y.; Ayokoyama; Hirai, T.; Hirasawa, Y. (1998): Mechanism of lateral tibial plateau fracture analyzed by dispersion of stress wave. In *Proceeding of Third World Congress of Biomechanics*, pg. 245a. August 2-8, Sapporo, Japan.